AARMS
Volume 1, Issue 2 (2002) 253–269

TECHNOLOGY

Robustness stability and robust performance of the automatic flight control systems

RÓBERT SZABOLCSI, PÉTER SZEGEDI

Miklós Zrínyi National Defence University, Department of Aircraft Onboard Systems, Szolnok, Hungary

This paper deals with the analysis of the robustness stability and robust performance of the pitch rate stability augmentation system. Dynamics of the fuselage elastic bending motion will be considered for additive uncertainty. The purpose of the authors is to analyze if the given controller is able to stabilize the aircraft motion when its true dynamics is taken into account during controller gain selection.

1. Introduction

This paper summarizes some of the methods available for robustness analysis of the single input – single output (SISO) and multi input – multi output (MIMO) control systems. Two methods of uncertainty modeling will be presented. The goal of the authors was to analyze if the flight control system's controller is able robustly stabilize the system.

The paper is organized the following manner. In Section 2 dynamic performances of the SISO control systems are derived. Section 3 is for the derivation of the dynamic performances of the MIMO control systems. In Section 4 we deal with uncertainty modeling. Conditions and main equations of robust stability are presented in Section 5. Mathematical model of the elastic motion and the aircraft longitudinal motion are given in Section 6. In this section basic data for analysis of the longitudinal stability augmentation are also given. Section 7 and 8 are for time and frequency domain analysis of the pitch rate damper. Results of computer simulation of the robustness analysis are given in Section 9. This paper ends with some closing remarks, conclusions and references.

2. Dynamic performances of the SISO systems

In this section, we will describe basic equations of the SISO control systems. The block diagram of the SISO control system can be seen in Figure 1:[1, 11]

Received: September 26, 2002

Address for correspondence:
RÓBERT SZABOLCSI
Miklós Zrínyi National Defence University, Department of Aircraft Onboard Systems,
H-5008 Szolnok, POB. 1., Hungary
E-mail: drszr@solyom.szrfk.hu

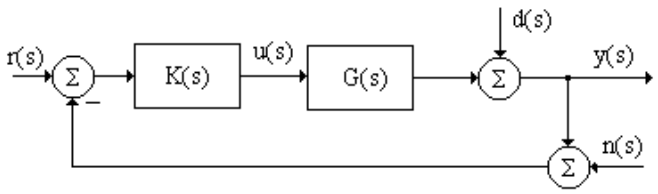

Figure 1. Block diagram of the SISO control system

In Figure 1 r(s) represents the reference signal, d(s) is the external disturbance, n(s) is the sensor noise, G(s) is the transfer function of the plant, K(s) is the transfer function of the controller, u(s) is the input vector, and, finally, y(s) is the output signal. Using Figure 1 the output signal y(s) can be derived as:

$$y(s) = \frac{K(s)G(s)}{1+K(s)G(s)}r(s) + \frac{1}{1+K(s)G(s)}d(s) - \frac{K(s)G(s)}{1+K(s)G(s)}n(s) \ . \tag{2.1}$$

In Eq. (2.1) let us introduce the following substitutions: $L(s) = K(s)G(s)$ – open loop transfer function, $S(s) = \frac{1}{1+K(s)G(s)}$ – sensitivity transfer function, $T(s) = \frac{K(s)G(s)}{1+K(s)G(s)}$ – closed loop complementary transfer function (closed loop transfer function).

Using the transfer function given above it is evident that

$$S(s) + T(s) = 1 \tag{2.2}$$

For achieving the prescribed reference signal tracking ability, the sensitivity transfer function S(s) must have small value in the given frequency domain, i. e., the open loop transfer function is large. For achieving the necessary noise suppressing ability, the sensitivity transfer function S(s) has small value in the frequency domain, in which the external disturbance d(s) acts.

Sensor noises are said to be well damped if the closed loop transfer function T(s) has small values in the given frequency domain, i. e., the open loop transfer function must have small value.

Bode diagrams of the sensitivity transfer function, S(s), and the closed loop complementary transfer function, T(s), can be seen in Figure 2.

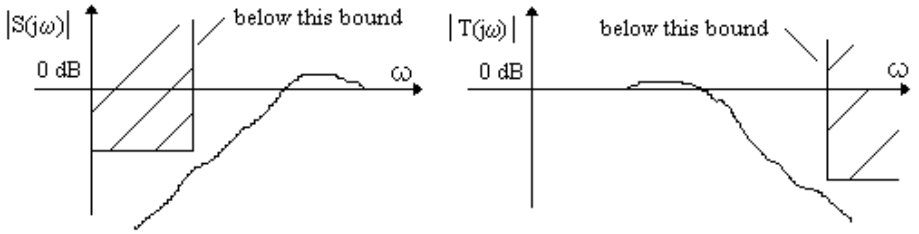

Figure 2. Bounds for $|S(j\omega)|$ and $|T(j\omega)|$

In low frequency domain $|S(j\omega)|$ must be kept small, while in high frequency domain its absolute value goes to unity. In low frequency domain $|T(j\omega)|$ must be kept unit value, in high frequency domain it is bounded for good noise suppressing ability.

For the SISO control system these simultaneous requirements determine the shape of the open loop Bode diagram as illustrated in Figure 3. In low frequency domain, in which the reference signal and the disturbance act, open loop gain must be kept large.

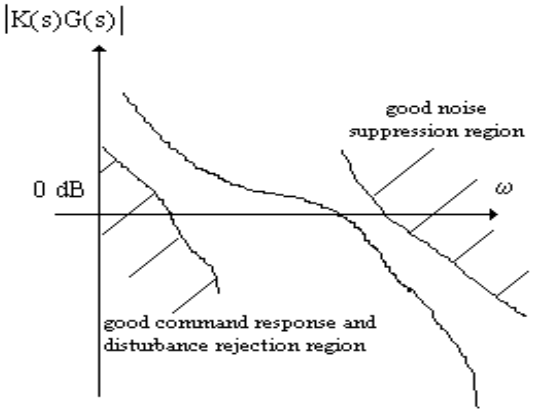

Figure 3. Desirable shape of the open loop system bode diagram

In high frequency domain open loop gain must be small for good noise suppressing ability. For the control of the gain and phase margins at the crossover, frequency slope of the Bode plot must be – 20 dB/decade.

3. Dynamic performances of the MIMO systems

The automatic flight control system is the MIMO one and the state space method must be applied for its analysis and design. In this case all input signals are vectors. In the MIMO control system we deal with the so-called transfer function matrices. For the evaluation of the size of matrices there is widely applied the *matrix singular value* method. For the MIMO control system Eq. (2.1) may be rewritten in following manner:

$$\mathbf{y}(s) = \frac{\mathbf{G}(s)\mathbf{K}(s)}{\left[\mathbf{I} + \mathbf{G}(s)\mathbf{K}(s)\right]}\mathbf{r}(s) - \frac{\mathbf{G}(s)\mathbf{K}(s)}{\left[\mathbf{I} + \mathbf{G}(s)\mathbf{K}(s)\right]}\mathbf{n}(s) + \frac{1}{\left[\mathbf{I} + \mathbf{G}(s)\mathbf{K}(s)\right]}\mathbf{d}(s)\,. \tag{3.1}$$

The sensitivity and the closed loop sensitivity transfer function matrices can be determined as follows:

$$\mathbf{T}(s) = \frac{\mathbf{G}(s)\mathbf{K}(s)}{\left[\mathbf{I} + \mathbf{G}(s)\mathbf{K}(s)\right]}; \mathbf{S}(s) = \frac{1}{\left[\mathbf{I} + \mathbf{G}(s)\mathbf{K}(s)\right]} \tag{3.2}$$

Nominal performance criterions for the SISO and the MIMO control systems are summarized in Table 1. Subscript 'm' denotes the largest singular values of the matrices.

Table 1. Nominal performance criterions for the SISO and the MIMO control systems

	Low frequency domain		High frequency domain	
	SISO	MIMO	SISO	MIMO
Reference signal tracking	$\lvert K(s)G(s)\rvert \gg 1$ or $\lvert S(s)\rvert \ll 1$	$\sigma(\mathbf{K}(s)\mathbf{G}(s)) \gg 1$ or $\sigma_m(\mathbf{S}(s)) \ll 1$		
Disturbance rejection	$\lvert K(s)G(s)\rvert \gg 1$ or $\lvert S(s)\rvert \ll 1$	$\sigma(\mathbf{K}(s)\mathbf{G}(s)) \gg 1$ or $\sigma_m(\mathbf{S}(s)) \ll 1$		
Noise suppression			$\lvert K(s)G(s)\rvert \ll 1$ or $\lvert T(s)\rvert \ll 1$	$\sigma_m(\mathbf{K}(s)\mathbf{G}(s)) \ll 1$ or $\sigma_m(\mathbf{T}(s)) \ll 1$

4. Uncertainty models applied in contol theory

Next we will discuss types of uncertainties to be considered later. Uncertainties can be divided into two categories: structured and unstructured ones. Structured uncertainty is the modeled one and has ranges and bounds on it. Unstructured uncertainty is the less-known one and its frequency response lies between two bounds. Unstructured uncertainty can be modeled in two different ways. One can discuss additive or multiplicative uncertainties. Let the nominal system model is denoted by $G(s)$. The actual true system is defined with $\tilde{G}(s)$. The actual system can be modeled as sum of nominal system plus the additive uncertainty model:[1, 10]

$$\tilde{G}(s) = G(s) + \Delta_a(s) \tag{4.1}$$

From Eq. (4.1) the model of the additive uncertainty can be derived as:

$$\Delta_a(s) = \tilde{G}(s) - G(s). \tag{4.2}$$

Additive uncertainty can be represented using Eq. (4.1) and it can be seen in Figure 4.

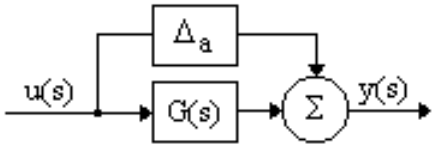

Figure 4. Additive uncertainty model

Additive uncertainty model is often used in automatic flight control system to model aeroelastic high frequency dynamics of the aircraft fuselage. Additive uncertainty represents absolute error in the model.

In the multiplicative uncertainty case one can find the true model of the system as:

$$\tilde{G}(s) = \left(1 + \Delta_m(s)\right)G(s) \tag{4.3}$$

Multiplicative uncertainty can be built using Eq. (4.3). It can be represented at the plant input or at the plant output. Block diagram of multiplicative uncertainty can be seen in Figure 5.

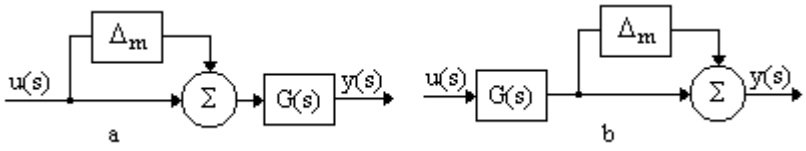

Figure 5. Multiplicative uncertainty model
'a' – uncertainty at the plant input, 'b' – uncertainty at the plant output

Multiplicative uncertainty represents relative error in the model and it is used more often than additive one.

5. Robust stability of control systems

Let us consider a feedback control system containing a plant and the compensator designed for the nominal plant $G(s)$. The compensator *robustly* stabilizes the system if the closed loop control system remains stable for the true plant $\tilde{G}(s)$.

Robust stability conditions can be derived from variation of the Nyquist stability criterion or from the so-called *small-gain theorem*. This theory states that, for the closed loop stability the open loop gain $|G(s)K(s)|$ is small.[6–9] The small-gain theorem guarantees internal stability. It means that all possible closed loop transfer functions are stable and all internal signals are bounded for bounded inputs.

From Section 2 it is known that for good command performance and for good disturbance rejection in the low frequency domain the open loop gain must be larger than one. Hence, the control system satisfying this theorem will have poor dynamic performances. Inspite of this it is possible to apply the small-gain theorem for control systems with additive and multiplicative uncertainties.

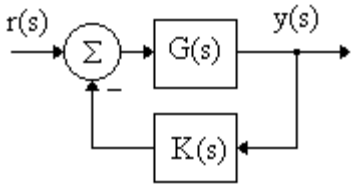

Figure 6. Feedback control system

The small-gain theorem is mainly used for answering the following two questions. The first is, if the given uncertainty is stable and bounded will the closed loop system be stable for this uncertainty? The second one is, for the given control system what is the smallest uncertainty destabilizing the closed loop control system?

Consider a system with nominal plant $G(s)$ and the compensator. The plant and the compensator are supposed to be stable ones.

Using the Nyquist stability criterion the closed loop control system is stable if and only if the following inequality holds:

$$\left|G(s)K(s)\right| < 1. \tag{5.1}$$

Left side of the inequality (5.1) can be rewritten as

$$\left|G(s)K(s)\right| \le \left|G(s)\right|\left|K(s)\right| \tag{5.2}$$

The closed loop stability condition can be derived from Eqs. (6.1) and (6.2). We have for this criterion:

$$\left|G(s)\right|\left|K(s)\right| < 1. \tag{5.3}$$

Let us use the small-gain theorem for derivation of conditions of robust stability of control system under multiplicative uncertainty at the plant output. Consider the feedback system shown in Figure 7a. To derive the block diagram of the feedback system in Figure 6 it is necessary to determine the transfer function seen by the uncertainty. For this refer to Figure 7b and the transfer function M(s) (see Figure 7c) between 'input' and 'output' is given by the following formula:

$$M(s) = \frac{-G(s)K(s)}{1+G(s)K(s)}. \tag{5.4}$$

The small-gain theorem states that if the transfer function (5.4) and the uncertainty transfer function are stable the closed loop control system will be robustly stable if and only if

$$\left|\Delta_m(s)\right| < \frac{1}{\left|G(s)K(s)\left[1+G(s)K(s)\right]^{-1}\right|}, \tag{5.5}$$

or, in other form,

$$\left|\Delta_m(s)\right| < \frac{1}{\left|T(s)\right|}. \tag{5.6}$$

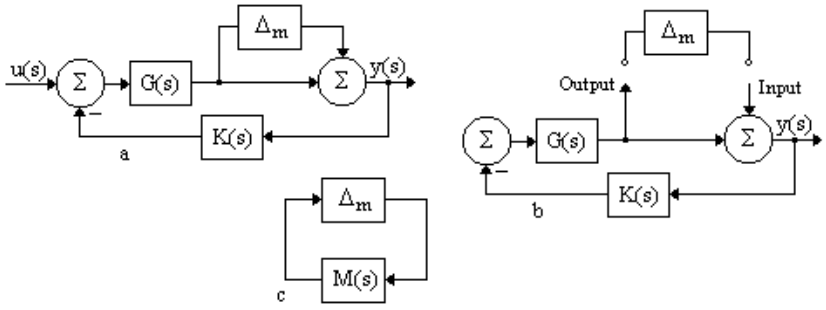

Figure 7. Feedback control system with multiplicative uncertainty

Eqs (5.5) and (5.6) can be used to answer the first of the two questions posed earlier. If the uncertainty is bounded by the given scalar γ, one can have the following inequality:

$$|T(s)| < \frac{1}{\gamma}, \text{ or } |\gamma\, T(s)| < 1. \tag{5.7}$$

The second question of two posed before is about finding the smallest stable multiplicative uncertainty, which will destabilize the closed loop system. It is known that uncertainty must be smaller than $\frac{1}{|T(s)|}$, i. e., it must be smaller than the minimum of $\frac{1}{|T(s)|}$. For the minimum of the left side of Eq. (5.6) we must maximize $T(s)$. The maximum of $T(s)$ over all possible frequencies is its peak value. The smallest uncertainty destabilizing the feedback system is given by

$$\text{MSM} = \frac{1}{M_r}, \text{ where } M_r = \sup_{\omega} |T(j\omega)|. \tag{5.8}$$

In Eq. (5.8) *MSM* denotes the *Multiplicative Stability Margin*. The *supremum* of $|T(j\omega)|$ is equal to the maximum of the function when the maximum is attained.

For the MIMO feedback system the size of the smallest destabilizing multiplicative uncertainty can be derived as follows:

$$\bar{\sigma}[\Delta_m(j\omega)] = \frac{1}{\bar{\sigma}[T(j\omega)]}. \tag{5.9}$$

Using the same approach the conditions of robust stability under additive uncertainty can be determined. Transfer function seen by the uncertainty is given by

$$M(s) = \frac{-K(s)}{1 + G(s)K(s)}. \tag{5.10}$$

The feedback system will be robustly stable if takes place the following inequality:

$$\left|\Delta_a(s)\right| < \frac{1}{\left|K(s)\left[1 + G(s)K(s)\right]^{-1}\right|}, \tag{5.11}$$

or in other manner

$$\left|\Delta_a(s)\right| < \frac{1}{\left|K(s)S(s)\right|}. \tag{5.12}$$

If the additive uncertainty is stable and bounded by

$$\left|\Delta_a(s)\right| < \frac{1}{\gamma}. \tag{5.13}$$

The closed loop robust stability can be guaranteed if

$$\left|K(s)S(s)\right| < \frac{1}{\gamma}, \text{ or } \left|\gamma\, K(s)S(s)\right| < 1. \tag{5.14}$$

The *Additive Stability Margin (ASM)* can be defined by

$$ASM = \frac{1}{\sup\limits_{\omega}\left|K(j\omega)S(j\omega)\right|}. \tag{5.15}$$

For the MIMO feedback system the size of the smallest additive uncertainty destabilizing the feedback system can be derived as follows:

$$\overline{\sigma}\left[\Delta_a(j\omega)\right] = \frac{1}{\overline{\sigma}\left[K(j\omega)S(j\omega)\right]}. \tag{5.16}$$

It is easily can be seen that for protection against destabilizing multiplicative uncertainties MSM must be large, the complementary sensitivity must be small. It leads to good noise suppression but conflict with reference signal tracking and disturbance rejection. The transfer function of ASM is that of determining control energy.

6. Mathematical model of the elastic aircraft

In this section we will describe mathematical model of the elastic aircraft. There are many scientific papers and textbooks dealing with principle of aeroelasticity.[2,4,5] Two main methods are available for deriving mathematical model of the elastic aircraft. The first one is the state space method. The second one is the transfer function method. In this work we will focus our attention to the transfer function method.

In general, elastic motion of the aircraft fuselage generated by angular deflection of the elevator can be defined using following formula:[5]

$$\omega_{Z_E}(s) = \sum_{i=1}^{\infty} \frac{sK_i}{s^2 + 2\xi_i \omega_i s + \omega_i^2} \delta_E(s), \tag{6.1}$$

where $\delta_E(s)$ represents angular deflection of the elevator, K_i is the gain of the *i*th elastic degree of freedom, ω_i is the natural frequency and, ξ_i is the damping ratio of the *i*th elastic degree of freedom, respectively. Let us consider parameters of the 1st and the 2nd overtones of the fighter fuselage bending motion given as follows:[5]

$$K_1 = 10\,s^{-2},\ \omega_1 = 10\,s^{-1},\ \xi_1 = 0{,}05;\ K_2 = 5\,s^{-2},\ \omega_2 = 20\,s^{-1},\ \xi_2 = 0{,}02 \tag{6.2}$$

It is supposed that the longitudinal motion control system is affecting only the short period motion. The simplified mathematical model of the longitudinal motion of the aircraft is given by:[2,3,5]

$$\omega_{Z_R}(s) = -\frac{A(1 + sT_\theta)\omega_\alpha^2}{s^2 + 2s\xi_\alpha \omega_\alpha + \omega_\alpha^2} \delta_E(s) \tag{6.3}$$

In Eq. (6.15) – for the flight conditions H=1000 m and M=0.4 – let us consider the following parameters of the aircraft:

$$A = 1{,}5\,s^{-1};\ T_\theta = 2\,s;\ \omega_\alpha = 5\,s^{-1};\ \xi_\alpha = 0{,}5 \tag{6.4}$$

The resulting output signal of the pitch rate gyro can be determined as a sum of the rigid and elastic aircraft output signals defined by eqs (6.1) and (6.3):

$$\omega_Z(s) = \omega_{Z_E}(s) + \omega_{Z_R}(s) \tag{6.5}$$

7. Time domain analysis of the longitudinal stability augmentation system

Let us consider the aircraft model defined by eqs (6.2) and (6.4). Eigenvalues and dynamic performances of the aircraft are as follows:

$$\lambda_{1,2} = -2{,}5 \pm 4.33\mathrm{i},\ \xi = 0.5,\ \omega = 5\mathrm{rad/s} \tag{7.1}$$

Dynamic performances of the uncontrolled aircraft are different from the desired ones given above. Aircraft damping ratio during its controlled flight must be between 0,6 and 0,8 [12]. For providing desirable dynamic performances the pole placement must be used. Pole placement is realized using state feedback by the pitch rate, which is available for measurement. The pitch rate damper is built using sensor, controller and hydraulic actuator. In conventional stability augmentation systems the pitch rate sensor is the electro-mechanical device. Sensor dynamics can be represented as the proportional second order term. Assuming high natural frequency of the pitch rate gyro it can be modeled as a simple proportional term with unity gain K_s. The compensator is supposed to be proportional term and denoted by K_c. During analysis of the pitch rate it is supposed that hydraulic actuator has fast response to input signals without any time delay. The block diagram of the longitudinal stability augmentation of the elastic aircraft can be seen in Figure 10.

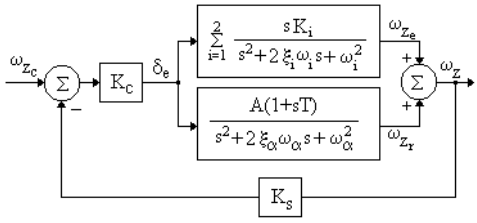

Figure 10. Longitudinal motion stability augmentation system

The uncontrolled and the controlled aircraft was analyzed in the time domain. The result of the computer simulation can be seen in Figure 11.

From Figure 11 it can be seen that the uncontrolled aircraft transient response has large overshoot and response time. The controlled rigid aircraft has faster response without overshoot. Dynamic performances of the closed loop system were determined and they are as given by:

$$\lambda_1 = -0.757,\ \lambda_2 = -7.92,\ \xi_1 = \xi_2 = 1,\ \omega_1 = 0.757\mathrm{rad/s},\ \omega_2 = 7.92\mathrm{rad/s}. \tag{7.2}$$

The closed loop perturbed control system was analyzed in the time domain. Results of the computer simulation can be seen in Figure 12. From Figure 12 it can easily be seen that the first and the second overtones lead to oscillation of the pitch rate step response.

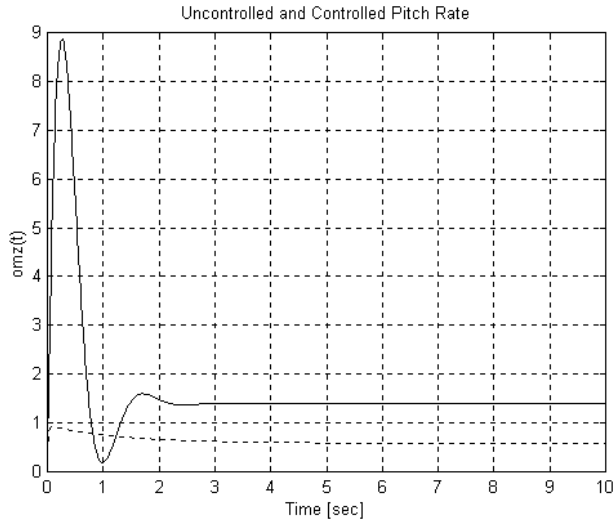

Figure 11. Pitch rate step responses.
Solid: uncontrolled aircraft, dash and grid: controlled aircraft

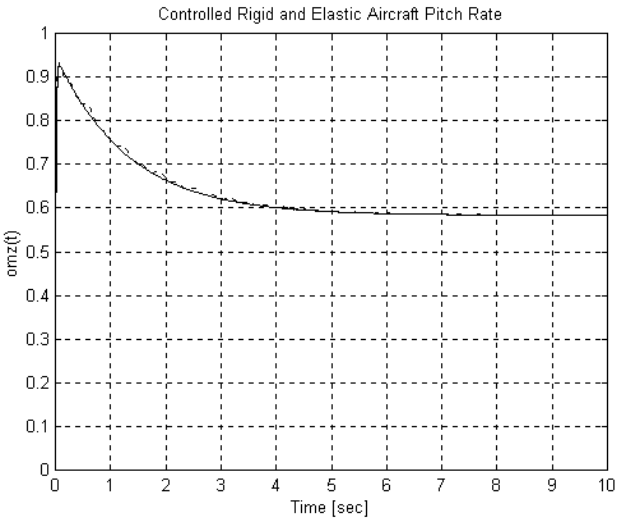

Figure 12. Pitch rate responses.
Solid: rigid aircraft, dash and grid: elastic aircraft

8. Frequency domain analysis of the longitudinal stability augmentation system

Robust stability analysis gives answer to question if controller is able to stabilize the true plant? Firstly, let us analyze the frequency domain behavior of the additive uncertainty. Bode diagram of the additive uncertainty represented by the high frequency dynamics of the aircraft elastic motion can be seen in Figure 13.

Uncertainty gain has resonance peak at 10 and at 20 rad/s developed by the D-term in the numerator of Eq. (6.1). Both in low and in high frequency domain the uncertainty gain is small.

The additive uncertainty affects the frequency domain behavior of the open loop stability augmentation system. Results of the computer simulation can be seen in Figure 14.

Form Figure 14 it can be seen that at the resonance frequencies of 10 and 20 rad/s the gain and the phase angle have peaks in their values. The open loop gain and the phase angle are increased only at the resonance frequency and in its vicinity.

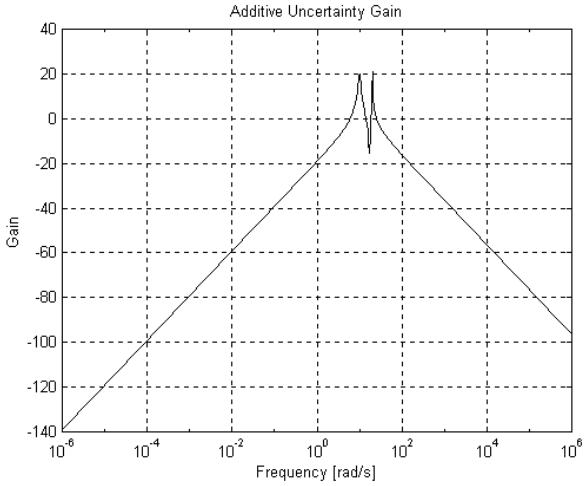

Figure 13. Additive uncertainty Bode diagram

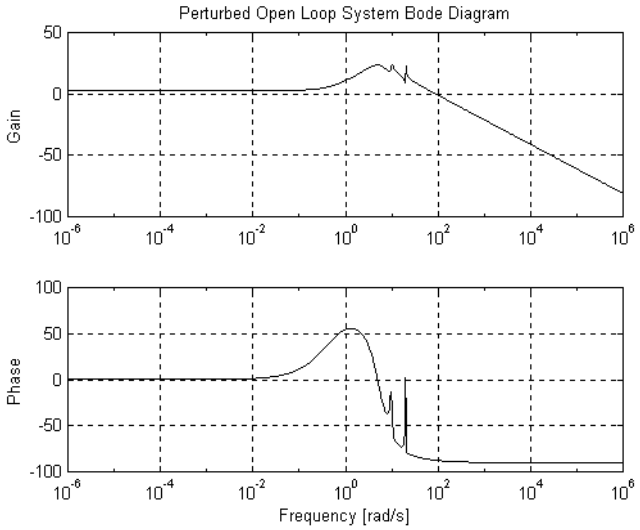

Figure 14. Bode diagram of the open loop perturbed system

9. Robustness analysis of the longitudinal stability augmentation system

Basic equations of robustness analysis of the control systems were summarized in Section 5. The sensitivity transfer function S(s) and the closed loop complementary transfer function T(s) were derived. Their frequency domain behavior was analyzed and it can be seen in Figure 15.

From Eq. (5.16) it is evident that the closed loop system can be said robustly stable if inverse of the sensitivity transfer function larger than the additive uncertainty gain. This condition was analyzed and the closed loop system was tested for this inequality. Results of the computer simulation can be seen in Figure 16.

From Figure 16 it is evident that inverse of the sensitivity transfer function – for the unity gain of the sensor – due to second overtone of the aircraft elastic motion is less than the additive uncertainty gain. It means that the closed loop control system of the pitch rate damper is robustly unstable. If to consider only the first elastic overtone the closed loop pitch rate damper is robustly stable. Because of the dynamic performances of the first and the second overtones i. e., the gains, damping ratios and natural frequencies in flight control systems it is regarded to take into account both of them simultaneously. In some cases the output electrical signal of the pitch rate sensor is filtered using passive or active filters.

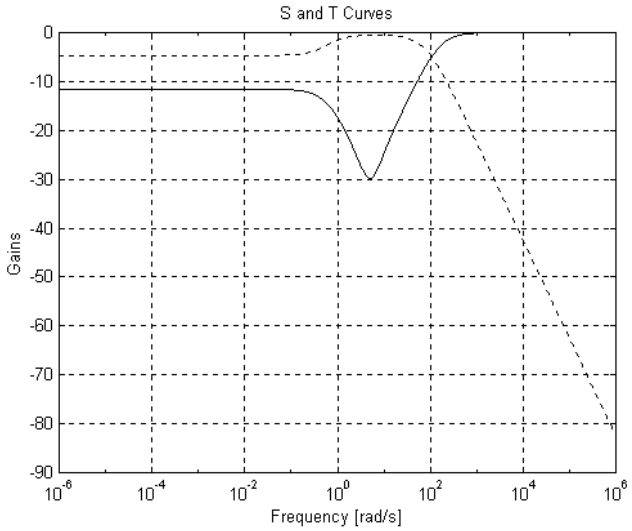

Figure 15. The sensitivity and the closed loop complementary transfer functions.
Solid: 'S', dash and dot: 'T'

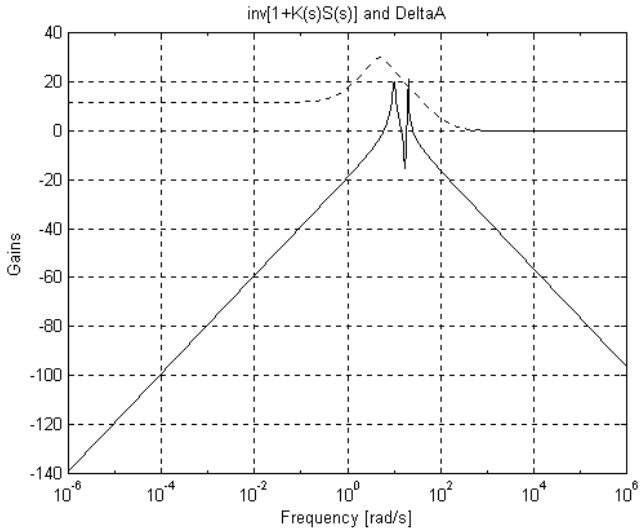

Figure 16. The inverse sensitivity transfer function and the additive uncertainty gain.
Dash and dot: 'inv[1+K_s(s)S(s)]'; solid: 'Additive Uncertainty Gain'

10. Summary and conclusions

The paper dealt with dynamic performances of the SISO and MIMO feedback systems and its main equations. The sensitivity and closed loop sensitivity transfer functions have been involved to determine the desirable shape of the open loop Bode diagram. Shapes of these functions were determined so as to meet dynamic performances of the feedback system. Two kinds of uncertainties were presented for determination if controller is able robustly stabilize the true plant with given uncertainty. For derivation of smallest uncertainty destabilizing the closed loop control system the multiplicative and additive stability margins also were determined. Basic equations of the aircraft elastic motion and its transfer function were derived. The high frequency dynamics generated by elevator angular deflection have been involved as additive uncertainty. The closed loop control system of the aircraft longitudinal stability augmentation system was analyzed for the 1^{st} and the 2^{nd} overtones of the fuselage elastic motion. The transient behavior, Bode diagrams and the dynamic performances were derived and analyzed. The robust stability was determined using condition for the inverse of the sensitivity transfer function and the resulting additive uncertainty gain. It must be stated that for the given uncertainties involved in this task for providing robust stability it is necessary to filter the pitch rate sensor output signal.

*

This research work has been supported by Széchenyi István Professorship of Ministry of Education under grant N^0 175/2001, which is gratefully acknowledged by the authors.

References

1. SHAHIAN, B., HASSUL, M.: *Control System Design using MATLAB®,* Prentice-Hall, Englewood Cliffs, New Jersey, 1993.
2. MCLEAN, D.: *Automatic Flight Control System*, Prentice-Hall, 1990.
3. SZABOLCSI, R.: D*esign of the Pitch Attitude Control System for the Aeroelastic Fighter Aircraft,* Bulletins for Applied Mathematics, BAMM-1240/96, LXXX., pp. (29-40), Göd, Hungary, 10-13 October, 1996.
4. BISHPLINGHOFF, R. L., ASHLEY, H.: *Principles of Aeroelasticity*, John Wiley & Sons, Inc., New York, London, 1962.
5. KRASOVSKY, A. A. et al.: *Aircraft Automatic Flight Control Systems*, Joukowsky Military Academy, Moscow, 1986 (in Russian).
6. MACIEJOWSKI, J. M.: *Multivariable Feedback Design*, Addison-Wesley Publishing Company, 1989.

7. DAHLEH, M. A., DIAZ-BOBILLO, I. J.: *Control on Uncertain Systems – A Linear Programming Approach*, Prentice-Hall, Englewood Cliffs, 1995.
8. WEINMANN, A.: *Uncertain Models and Robust Control*, Springer-Verlag, Wien-New York, 1991.
9. MORARI, M., ZAFIRIOU, E.*: Robust Process Control*, Prentice-Hall International, Inc., 1996.
10. SZABOLCSI, R., SZEGEDI, P.: *Robustness Analysis of Control Systems*, Proceedings of the Pannonian Applied Mathematical Meetings PAMM, PC-136 Conference, 24-27 January, 2002 (in Print).
11. SZABOLCSI, R., SZEGEDI, P.: *Robustness Analysis of the Flight Stability Augmentation Systems*, Proceedings of the Pannonian Applied Mathematical Meetings PAMM, PC-136 Conference, 24-27 January, 2002 (in Print).
12. MIL-F-8785C *Flying and Handling Qualities of Piloted Airplanes*, 1980.